JACS
JOURNAL OF THE AMERICAN CHEMICAL SOCIETY
Article
pubs.acs.org/JACS

Phase Separation Polymerization of Dicyclopentadiene Characterized by In Operando Fluorescence Microscopy

Eva M. Hensle and Suzanne A. Blum*

Department of Chemistry, University of California, Irvine, California 92697-2025, United States

Supporting Information

ABSTRACT: Phase separation polymerization of dicyclopentadiene has been characterized from initiation to bulk material formation for the first time via in operando fluorescence microscopy imaging. The morphology of the precipitated polymers at early reaction stages persists in the bulk polymer after completion of the reaction. Two-fluorophore experiments revealed the mechanistic origin of the "dumbbell" morphology as physical strand aggregation/precipitation rather than chemical attachment and revealed that strand aggregation was slow and irreversible relative to precipitation. These data highlight the complementary information available through the single-particle sensitivity and in operando microscopy nature of this technique.

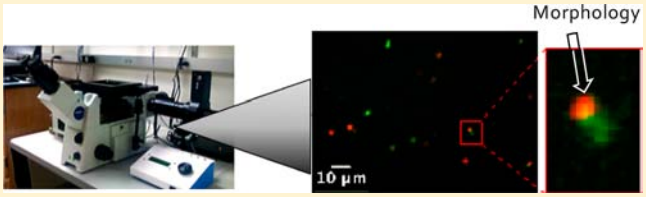

INTRODUCTION

Phase separation polymerization is a critical mechanistic hypothesis that is proposed to yield desirable bulk-polymer properties for diverse applications including ion exchange resins,[1] size exclusion chromatography,[1,2] catalyst support materials,[1−4] and matrices for tissue engineering.[4] Yet the mechanism of polymerization (i.e., phase separation, traditional network polymerization, or combination of the two) is challenging to characterize.[5] Complicating this characterization, a general in operando microscopy technique for imaging phase separation polymerization does not exist.[6] SEM[1−3,8−11] and TEM[9,11,12] measurements are often applied to examine polymer precipitation and morphology; however, these techniques require quenching the reaction or removing aloqates, processes that have the possibility to induce artifacts.[20,21]

We now present a general in operando fluorescence microscopy technique for imaging the phase separation polymerization processes. Images acquired through this technique provided the first real-time phase separation observation in dicyclopentadiene **1** (DCPD) polymerization from initiation to bulk material formation. PDCPD, a tough and rigid thermoset polymer, was chosen for this study because of its industrial applications arising from its robustness and chemical and corrosion resistance.[22−25] The single-particle sensitivity and time resolution of the technique permitted following the same individual polymer particles through the course of reaction. These images: (1) reveal phase separation as a critical component of midstage DCPD polymerization, (2) characterize previously unknown spherical and "dumbbell" morphologies of initial PDCPD aggregates, (3) disclose the mechanism for formation of the dumbbell morphologies as aggregation of two preformed polymer particles, (4) demonstrate that these initial morphologies partially persist in the bulk polymer, and (5) reveal a mechanism for polymer growth in which precipitated polymers were not susceptible toward further monomer incorporation. These insights would not be available through a traditional bulk material ensemble measurement or a measurement that required removal and/or quenching of alloquats.

RESULTS AND DISCUSSION

A schematic of the in operando microscopy imaging of DCPD polymerization is shown in Figure 1c. A sample of Grubbs II catalyst (**4**), heptane cosolvent, one or both of the different colored fluorescent boron dipyrromethene (BODIPY) green **2** or orange **3**, and DCPD were added to a reaction vial fitted with a microscope coverslip bottom. The growing polymers became chemically tagged with green or orange fluorophores via olefin metathesis and thus became imageable by sensitive fluorescence microscopy in total internal reflection fluorescence (TIRF) mode.[26] The single-fluorophore sensitivity of this technique permits the detection of as little as one tag per polymer; however, precipitated polymers contained multiple tags per particle[27−30] consistent with strand aggregation. After ∼1 min, phase separation/precipitation of PDCPD began (Figure 1a) and initially the shapes of the phase separated polymers appeared as spheres of diameter ∼0.5−7 μm. At increasing reaction times, polymers with multiball morphology were observed akin to colloquial "dumbbell" shapes.

Two mechanistic hypotheses for the generation of these dumbbell morphologies were considered: (1) physical aggregation of two preformed spherical polymer particles or (2) chemical growth of an additional polymer from one preformed spherical polymer particle that retained catalytic activity and thus the ability to grow by incorporating monomer

Received: May 25, 2013
Published: July 25, 2013

   dx.doi.org/10.1021/ja405283k | J. Am. Chem. Soc. 2013, 135, 12324−12328

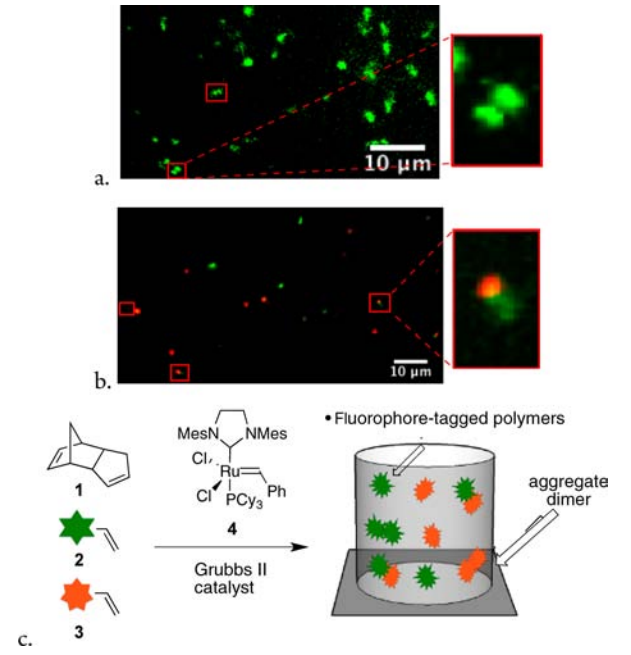

Figure 1. (a) Fluorescence microscopy image of DCPD polymerization at t = 187 s showing dumbbell morphology of polymer particles (examples in red boxes). (b) Mixing experiment of DCPD polymerization using both fluorophores **2** and **3** revealed that aggregation of two preformed polymer particles is responsible for the dumbbell formation. (c) Experiment schematic. In operando microscopy imaging of phase separation in DCPD polymerization.

(via a living polymerization or "bead-on-a-string" polymerization process).

To differentiate between these two hypotheses, a two-color mixing experiment was performed. Polymerization was initiated in two separate vials simultaneously: one vial with green BODIPY tag **2** and a separate vial with orange BODIPY tag **3** (Figure 2). The reaction conditions were identical with the

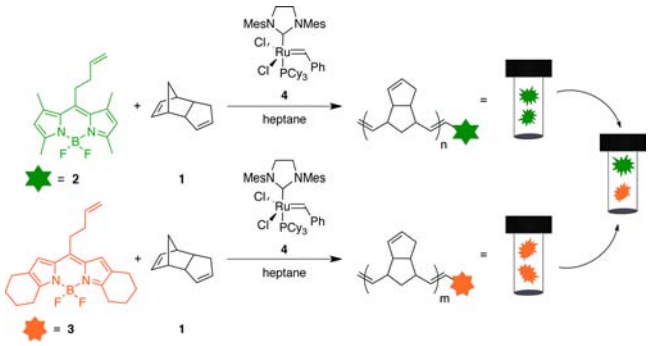

Figure 2. Polymerization of DCPD via ring-opening metathesis tagged with one color each of the fluorescent BODIPY tags in separate vials, followed by combination of the two polymerization mixtures.

exception of the color of the tag. After 2 min, the two polymerization mixtures (containing polymer particles of purely green or purely orange, respectively) were combined into one microscope reaction cell. If hypothesis 1 is correct, then aggregation of two preformed spherical polymers should occur in a statistical ratio that produces green−green, green−orange, and orange−orange dumbbell shapes. If, however, hypothesis 2 is correct, then subsequent growth off of existing spheres should have an equal chance of incorporating green and orange BODIPY tags, which are now *both* present. The mixed incorporation portion would appear as yellow, yielding green−yellow and orange−yellow dumbbell shapes. Success of this differentiation experiment would require phase separation to occur faster than strand separation/aggregation equilibria that would scramble the colors (observable as completely yellow rather than discrete green and orange sections).

Images of the subsequent precipitation of PDCPD in the two-color experiment are shown in Figure 1b. The presence of green−green, green−orange, and orange−orange dumbbells demonstrated that hypothesis 1, aggregation, is responsible for generating the morphology. Within the first minute after mixing ∼20% of the precipitated polymers with dumbbell morphologies were mixed orange−green, with the remainder green−green and orange−orange. The under-representation of green−orange (expected at 50% from pure mixing statistics) is attributed to a subset of these same color combinations forming during the 2 min prior to mixing the contents of the two vials.

Two control experiments were consistent with the conclusion that physical aggregation rather than chemical cross-linking was responsible for the aggregate morphology (Figure 3). First, a control experiment employing norbornene

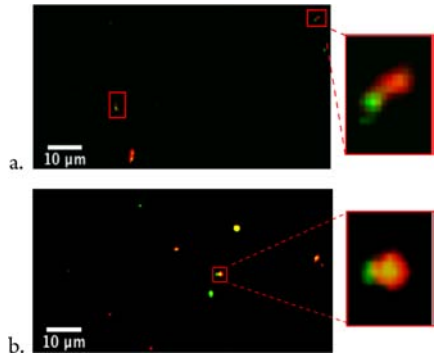

Figure 3. Control experiments for assignment of aggregation rather than chemical reaction of spherical polymer particles. (a) Norbornene was used as monomer instead of DCPD. (b) Quenching of the two polymerization mixtures with ethyl vinyl ether prior to combining them.

in the place of DCPD also yielded mixed colored dumbbell shapes despite the absence of a second double bond in norbornene capable of chemical cross-linking as could occur with DCPD (Figure 3a). Second, quenching the catalysts in both of the separate polymerizations with green BODIPY **2** and orange BODIPY **3** with ethyl vinyl ether, a known catalyst poison,[31] prior to combination of the reaction mixtures still yielded mixed color polymers (Figure 3b). Therefore, two-color aggregates still formed in the absence of an active catalyst for chemical linking.

Thus the mechanisms of the phase separation and the origin of nonspherical morphologies were both revealed to be physisorption/aggregation by this microscopy technique. The relative rate of strand dissociation/reaggregation was concurrently established to be slower than the precipitation process (eq 1) because colored aggregates did not scramble prior to precipitation. Thus strand aggregation/dissociation was not in equilibrium prior to the fast precipitation step.

Phase separation polymerization mechanisms have been demonstrated to give rise to macroscale properties for certain

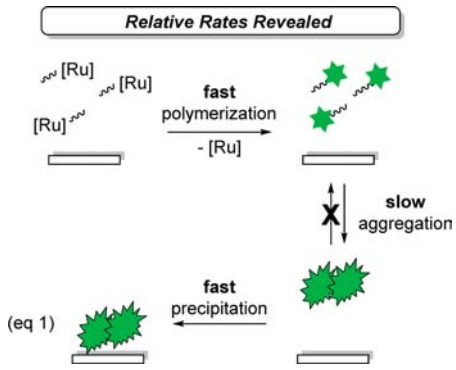

polymers.[1−5,32,33] We therefore asked the question whether the morphology of polymers during this specific phase separation was retained in the bulk material. Ethylidene norbornene (ENB) (5 wt %) was necessary as a comonomer to decrease the melting point of the mixture relative to neat DCPD and permit monitoring the neat bulk polymerization from the beginning to end with the microscope.[34] The absence of solvent in this experiment was analogous to the neat industrial polymerization conditions.[35,36]

Figure 4a shows the image of the neat bulk polymerization at t = 8 min, in which two polymer spheres were formed and

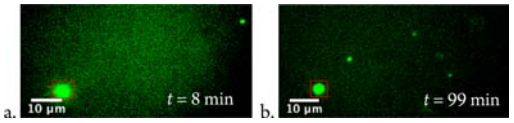

Figure 4. Bulk polymerization of neat DCPD with 5 wt % of ethylidene norbornene; early formed particle shape at t = 8 min (a) is still intact after complete polymerization at t = 99 min (b).

detected. One of these polymer particles, marked by a rectangle, retained its morphology and can still be detected at t = 99 min after the polymerization was complete (Figure 4b). Additional percipitated polymer particles were formed at later times and also preserved (Figure 4b; full movie available in Supporting Information, SI). These results demonstrate that bulk PDCPD with ENB is partially made up of individual polymer aggregates and therefore not exclusively a traditional network polymer with a continuous structure. The role that this microstructure plays in the bulk material properties is yet unclear. Because of photobleaching of the fluorophore molecules with time, the image of Figure 4b, after t = 99 min, is dimer compared to Figure 4a, polymerization after t = 8 min.

A "time-stamp" or "pulse-quench" experiment revealed when individual aggregates formed and phase separated. In this experiment, polymers that formed and phase separated within the first 2.4 min appeared green, and polymers that formed and phase separated between 2.4 and 5 min appeared orange (Figure 5). Specifically, polymerization of DCPD in heptane was started in the presence of only the green BODIPY fluorophore **2**. Thus, polymers that aggregated and/or precipitated at early reaction times were tagged green. After 2.4 min, most of the reaction mixture was removed, and a solution of DCPD in heptane containing the orange BODIPY dye **3** was added. Thus, polymers that aggregated and/or precipitated after 2.4 min were tagged orange. The sensitivity of fluorescence and single-particle microscopy resolution thus

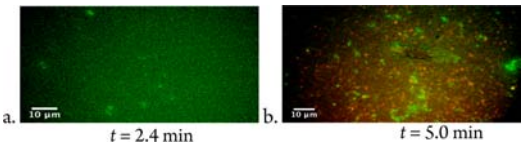

Figure 5. Time-stamp experiment: color of polymer shows time of synthesis/precipitation polymerization process. Polymerization at (a) t = 2.4 min: early polymer aggregates are green in 92 × 57 μm fluorescence images and (b) t = 5 min: later synthesized/aggregated/precipitated polymers are orange in 112 × 65 μm fluorescence images.

provided a color-coding technique to trace the time-of-formation of otherwise identical polymers.

The imaging technique also provided quantitative information on the number and size of the precipitated polymers at given time points in the polymerization process (Figure 6). At

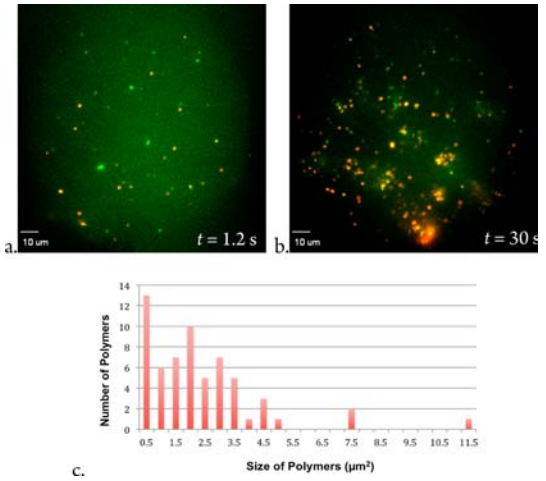

Figure 6. (a) Full-frame, 137 × 137 μm, fluorescence image of mixing polymerization experiment; at t = 1.2 s well-defined spherical polymers and two-color dumbbell shapes were detectable. (b) Same surface region as in (a) but at t = 30 s; larger polymer aggregates of each color precipitated onto the surface. (c) Quantitative analysis of polymer size at t = 1.2 s.

the beginning of the polymerization, small polymers initially formed with an average size of ∼1.7 μm^2 along with few larger ones (Figure 6a; distribution histogram in 6c). Larger precipitated polymer particles formed at increased reaction time as shown in Figure 6b.

We next investigated if the polymer aggregates retained catalytic activity after precipitation. The goal of this experiment was to pinpoint the location of active ruthenium centers either retained on the polymers or soley in solution. A polymerization of DCPD was started without fluorophore, thus creating precipitated polymers that were not tagged with fluorophore and therefore not observable by fluorescence microcopy. After 60 min, a solution of BODIPY fluorophore **2** was added to the precipitated polymers to investigate if the nonobservable dark polymer particles would incorporate fluorophore and become observable. The single-molecule sensitivity of the instrument revealed the incorporation of individual molecules[37] of BODIPY **2** into the precipitated polymers; however, a control experiment with metathesis-inert BODIPY **5** showed identical incorporation. Thus the incorporation could arise solely from physical incoporation of the BODIPY fluorophore into the viscous polymer rather than via chemical reactivity.

dx.doi.org/10.1021/ja405283k | J. Am. Chem. Soc. 2013, 135, 12324−12328

These data are most consistent with the polymer particles being catalytically inactive after precipitation and with the mechanistic hypothesis that polymer chains aggregate after completion of polymerization rather than during polymerization. Thus the rate of polymerization and ruthenium release was revealed to be fast relative to aggregation and precipitation.

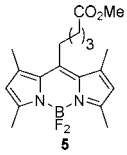

control, inert to olefin metathesis

5

Raman spectroscopy of the material obtained after completion of the fluorophore-tagging experiments confirmed the formation of PDCPD. Two observed bands at 1623 and 1664 cm^{-1} are characteristic for the C−C double bond of the cyclopentene ring and the double bond of the polymer backbone, respectively.[23] Differential scanning calorimetry (DSC) and thermogravimetric analysis (TGA) measurements of the bulk polymer provided a thermal decomposition of the material at around 490 °C and a glass transition temperature (T_g) of 181 °C. A similar decomposition temperature (495 °C) was reported for PDCPD in literature.[22] A range of T_g values has been reported for PDCPD that depends on and characterizes the amount of cross-linking. For reference, DSC measurements of linear PDCPD yielded a T_g of 53 °C.[38] The measured T_g of 181 °C for the material formed in our experiments indicates cross-linked material. This is consistent with the T_g range of 155 °C[36] to 259 °C[12] for cross-linked PDCPD obtained by reaction injection molding reported by Telene[36] and Yoonesi.[12]

CONCLUSION

In conclusion, the high sensitivity and single-particle resolution of fluorescence microscopy provided characterization of and mechanistic information about phase separation during the polymerization of DCPD.[39−43] The sensitivity of fluorescence microsopy permitted a small ratio of fluorophore to DCPD monomer (range $1{:}0.4 \times 10^6$ to $1{:}9 \times 10^9$ fluorophore:DCPD); thus the strand aggregation/precipitation processes are likely to be dominated by interactions between the polymer's DCPD backbone as occurs in the absence of the fluorophore, akin to normal academic and industrial conditions. The ability to resolve and follow individual polymer particles was critical to this technique's ability to reveal mechanisms of polymerization, determine relative rates of concurrent processes, provide real-time size distribution data, characterize morphologies of polymer precipitate, and unveil the mechanisms causing their shapes. These experiments highlight the complementary information available through this novel single-particle in operado imaging method compared to traditional SEM and TEM techniques.

ASSOCIATED CONTENT

Supporting Information

Synthetic methods, experimental protocols, data analysis, microscopy movies, and additional microscopy images. This material is available free of charge via the Internet at http://pubs.acs.org.

AUTHOR INFORMATION

Corresponding Author

blums@uci.edu

Notes

The authors declare no competing financial interest.

ACKNOWLEDGMENTS

We thank the U.S. Department of Energy, Office of Basic Energy Sciences (DE-FG02-08ER15994) for funding. We thank Ms. Olivia Cromwell for DSC and TGA measurements and Mr. Alexander Fast for Raman spectroscopy measurements.

REFERENCES

(1) Della Martina, A.; Garamszegi, L.; Hilborn, J. G. *J. Polym. Sci., Part A: Polym. Chem.* **2003**, *41*, 2036−2046.
(2) Della Martina, A.; Graf, R.; Hilborn, J. G. *J. App. Poly. Sci.* **2005**, *96*, 407−415.
(3) Kovačič, S.; Jeřábek, K.; Krajnc, P.; Slugovc, C. *Polym. Chem.* **2012**, *3*, 325−328.
(4) Busby, W.; Cameron, N. R.; Jahoda, C. A. B. *Biomacromolecules* **2001**, *2*, 154−164.
(5) Yu, Y.; Wang, M.; Gan, W.; Tao, Q.; Li, S. *J. Phys. Chem. B* **2004**, *108*, 6208−6215.
(6) In situ studies have been reported for the specific cases of spin-coating polymerization or for polymerization in a copolymer matrix; see refs 5, 7, 13−19.
(7) Toolan, D. T. W.; Howse, J. R. *J. Mater. Chem. C* **2013**, *1*, 603−616.
(8) Wan, X.; Xu, J.; Xie, X.-M.; Guo, B.-H. *Colloid Polym. Sci.* **2011**, *289*, 1719−1728.
(9) Knoke, S.; Korber, F.; Fink, G.; Tesche, B. *Macromol. Chem. Phys.* **2003**, *204*, 607−617.
(10) Amendt, M. A.; Chen, L.; Hillmyer, M. A. *Macromolecules* **2010**, *43*, 3924−3934.
(11) He, Y.; Yan, Y.; Zhang, L.; Zhu, S.; Zhang, Y. *Polym.-Plast. Technol. Eng.* **2011**, *50*, 1103−1108.
(12) Yoonessi, M.; Toghiani, H.; Kingery, W. L.; Pittman, C. U., Jr. *Macromolecules* **2004**, *37*, 2511−2518.
(13) Alg, I.; Steinhoff, B.; Lellinger, D. *Meas. Sci. Technol.* **2010**, *21*, 062001.
(14) Jisha, C. P.; Hsu, K.-C.; Lin, Y.-Y.; Lin, J.-H.; Chuang, K.-P.; Tai, C.-Y.; Lee, R.-K. *Opt. Mater. Express* **2011**, *1*, 1494−1501.
(15) Mok, M. M.; Torkelson, J. M. *J. Polym. Sci., Part B: Polym. Phys.* **2012**, *50*, 189−197.
(16) Nakanishi, H.; Namikawa, N.; Norisuye, T.; Tran-Cong-Miyata, Q. *Soft Matter* **2006**, *2*, 149−156.
(17) Van-Pham, D.-T.; Tran-Cong-Miyata, Q. *Adv. Nat. Sci.: Nanosci. Nanotechnol.* **2013**, *4*, 015003.
(18) Toolan, D. T. W.; Parnell, A. J.; Topham, P. D.; Howse, J. R. *J. Mater. Chem. A* **2013**, *1*, 3587−3592.
(19) Rajagopal, K.; Christian, D. A.; Harada, T.; Tian, A.; Discher, D. E. *Int. J. Poly. Sci.* **2010**, 379286.
(20) Little, B.; Wagner, P.; Ray, R.; Pope, R.; Scheetz, R. *J. Ind. Microbiol.* **1991**, *8*, 213−222.
(21) Wätjen, J. T.; Scragg, J. J.; Edoff, M.; Rubino, S.; Platzer-Björkman, C. *Appl. Phys. Lett.* **2013**, *102*, 051902.
(22) Constable, G. S.; Lesser, A. J.; Coughlin, E. B. *Macromolecules* **2004**, *37*, 1276−1282.
(23) Schaubroeck, D.; Brughmans, S.; Vercaemst, C.; Schaubroeck, J.; Verpoort, F. *J. Mol. Catal. A: Chem.* **2006**, *254*, 180−185.
(24) Mol, J. C. *J. Mol. Catal. A: Chem.* **2004**, *213*, 39−45.
(25) Kaplan, N.; Peled, G.; Bak, N. WIPO Patent WO 039737 A1, 2011.
(26) Esfandiari, N. M.; Blum, S. A. *J. Am. Chem. Soc.* **2011**, *133*, 18145−18147.
(27) Canham, S. M.; Bass, J. Y.; Navarro, O.; Lim, S.-G.; Das, N.; Blum, S. A. *Organometallics* **2008**, *27*, 2172−2175.
(28) Lim, S.-G.; Blum, S. A. *Organometallics* **2009**, *28*, 4643−4645.
(29) Esfandiari, N. M.; Wang, Y.; Bass, J. Y.; Cornell, T. P.; Otte, D. A. L.; Cheng, M. H.; Hemminger, J. C.; McIntire, T. M.;

Mandelshtam, V. A.; Blum, S. A. *J. Am. Chem. Soc.* **2010**, *132*, 15167−15169.
(30) Esfandiari, N. M.; Wang, Y.; McIntire, T. M.; Blum, S. A. *Organometallics* **2011**, *30*, 2901−2907.
(31) Choi, T.-L.; Grubbs, R. H. *Angew. Chem., Int. Ed.* **2003**, *42*, 1743−1746.
(32) Kara, S.; Pekcan, Ö. *Polymer* **2000**, *41*, 6335−6339.
(33) Brabec, C. J.; Heeney, M.; McCulloch, I.; Nelson, J. *Chem. Soc. Rev.* **2011**, *40*, 1185−1199.
(34) Gottschalk, D. M. Sc. Thesis, Iowa State University, 2011.
(35) Matějka, L.; Houtman, C.; Macosko, C. W. *J. Appl. Polym. Sci.* **1985**, *30*, 2787−2803.
(36) *Telene 1650 data sheet*; Telene Products, BF Goodrich: Charlotte, NC.
(37) Individual molecules exhibited the single-step photophysical processes that are well established "fingerprints" of individual molecules. See: Lakowicz, , J. R. *Principles of Fluorescence Spectroscopy*; Springer: New York, **2006**,.
(38) Abadie, M. J.; Dimonie, M.; Couve, C.; Dragutan, V. *Eur. Polym. J.* **2000**, *36*, 1213−1219.
(39) Weckhuysen, B. M. *Angew. Chem., Int. Ed.* **2009**, *48*, 4910−4943.
(40) Buurmans, I. L. C.; Weckhuysen, B. M. *Nat. Chem.* **2012**, *4*, 873−886.
(41) De Cremer, G.; Sels, B. F.; De Vos, D. E.; Hofkens, J.; Roeffaers, M. B. J. *Chem. Soc. Rev.* **2010**, *39*, 4703−4717.
(42) For an example of studying (an uncatalyzed) polymerization by single-molecule fluorescence microscopy, see: Wöll, D.; Braeken, E.; Deres, A.; De Schryver, F. C.; Uhi-i, H.; Hofkens, J. *Chem. Soc. Rev.* **2009**, *38*, 313−328.
(43) For examples of fluorescence microscopy used in polymerization catalysis see: (a) Titirici, M.-M.; Sellergren, B. *Chem. Mater.* **2006**, *18*, 1773−1779. (b) Jang, Y.-J.; Naundorf, C.; Klapper, M.; Müllen, K. *Macromol. Chem. Phys.* **2005**, *206*, 2027−2037. (c) Vriezema, D. M.; Hoogboom, J.; Velonia, K.; Takazawa, K.; Christianen, P. C. M.; Maan, J. C.; Rowan, A. E.; Nolte, R. J. M. *Angew. Chem.* **2003**, *115*, 796−800. (d) Tu, H.; Heitzman, C. E.; Braun, P. V. *Langmuir* **2004**, *20*, 8313−8320.